



QUASI-STATIC ANALYSIS OF MICROSTRIP LINES WITH INFINITELY THIN METALLIZATION THICKNESS

MIRJANA PERIĆ¹, ANA VUČKOVIĆ¹, NEBOJŠA RAIČEVIĆ¹

Keywords: Characteristic impedance; Effective relative permittivity; Finite element method; Hybrid boundary element method; Microstrip lines.

This paper presents a modified hybrid boundary element method (HBEM) approach for analysing microstrip lines with negligible metallization thickness. The proposed method enhances computational efficiency while maintaining high accuracy in determining transmission parameters such as characteristic impedance and effective permittivity. Numerical results validate the method's capability for analyzing both single and coupled microstrip lines with infinitely thin strip conductors, showing a maximum deviation of less than 1.3% from established approaches like the equivalent electrodes method (EEM) and finite element method (FEM). The developed approach enables the efficient modeling of microstrip structures where the conductor thickness is negligible, making it particularly useful in theoretical studies and the design optimization of microwave circuits, where metallization thickness has a minimal impact.

1. INTRODUCTION

In the field of microwave and millimeter-wave circuits, microstrip transmission lines are fundamental components, widely used in both commercial and military applications. Their compact size and efficient performance make them essential in high-frequency designs, including satellite communications, radar systems, and high-speed digital circuits [1–3]. However, the accurate modelling and analysis of microstrip lines are critical for optimizing circuit performance, particularly when considering variables such as strip conductor thickness. In many studies, the thickness of the strip conductor is often assumed to be negligible, allowing for a simplified analysis. For instance, Bryant and Weiss [4] utilized the dielectric Green's function to study coupled microstrip lines, where the strip thickness was assumed to be negligible. Many other studies have followed this trend, including the work by Nagel [5], which developed an analytical model for microstrip analysis using infinite series with mixed boundary conditions. This model assumes that strip conductors are infinitely thin – an approximation that is often valid in real-world scenarios due to the typically small strip thickness. Similarly, in [6], the spectral domain approach and Galerkin's technique are applied. Markov Chain Monte Carlo analysis was also in [7], for capacitance calculation of microstrip lines with the same assumption of negligible thickness.

The finite element method (FEM) has also been widely applied to model multiconductor transmission lines placed in multilayered dielectrics, as shown in [8]. Various microstrip line configurations have been analysed using the finite difference method in [9]. These studies continue to apply the assumption of negligible thickness for simplicity in microstrip design.

Despite the practical utility of assuming negligible strip thickness, there are many instances where this approximation is insufficient. As the width of the microstrip becomes comparable to the thickness of the strip conductor, the influence of the finite thickness on key transmission characteristics, such as characteristic impedance and effective permittivity, becomes significant.

To address this, several studies have focused on modifying classical methods to incorporate the finite strip thickness. In [10], the method of moments has been applied to analyse an outer-annular microstrip-fed antenna with the

finite metallization thickness of the microstrip line. The boundary element method (BEM) was extended in [11] by Chang and Tan to consider the effect of finite thickness, revealing that the impact of this thickness becomes noticeable when the strip width is small. These works highlight the importance of considering finite thickness, particularly in high-frequency designs [12].

Most of the mentioned studies apply a quasi-static transverse electromagnetic (TEM) approach, which is commonly used to analyse transmission lines in the low gigahertz frequency range. Such methods have been validated in numerous applications involving typical microstrip dimensions and substrate materials, where higher frequency effects can often be neglected [4]. However, these quasi-static approaches are limited when metallization thickness or other non-idealities become relevant, particularly as operational frequencies increase.

In [13], the influence of metallization thickness was analysed using the hybrid boundary element method (HBEM), considering both scenarios where the conductor penetrates the substrate and where it does not. The results of this analysis indicate that ignoring metallization thickness can lead to inaccuracies in certain instances, although it is often assumed to be negligible in practice.

The hybrid boundary element method, as introduced in [14], offers a semi-numerical approach to solving various electromagnetic problems. This method has been successfully applied to study electromagnetic field distributions near cable terminations [15] and to compute magnetic forces in permanent magnets [16]. It has also been employed to calculate the characteristic parameters of transmission lines [17,18] and has been utilized in the analysis of grounding systems [19].

During the application of HBEM for solving electrostatic and quasi-static problems, this methodology involves segmenting conductor surfaces and boundary interferences between dielectric layers into numerous segments, like the application of equivalent electrodes (EEs) within the equivalent electrodes method (EEM) [20]. Depending on the type of problem, *i.e.*, the analysed geometry, the equivalent electrodes may be line charges, toroidal electrodes, point charges, etc.

While the application of the HBEM mirrors EEM in problem scenarios where the Green's function of the considered problem is known, its distinctive utility emerges in complex multilayered systems, where the Green's

¹ Department of Theoretical Electrical Engineering, University of Niš, Faculty of Electronic Engineering, Aleksandra Medvedeva 4, Niš, Serbia.
E-mails: mirjana.peric@elfak.ni.ac.rs, ana.vuckovic@elfak.ni.ac, nebojsa.raicevic@elfak.ni.ac.rs

function is difficult or impossible to be found.

In previous applications [14,17], the HBEM approach was limited by its inability to fully address the distribution of polarization (bound) charges at conductor-dielectric layer boundaries. Early implementations only accounted for free charges on conductor surfaces, which limited the ability to calculate polarization charges distributions. This limitation was addressed in an enhanced version of HBEM, presented in [18], which introduced an improved method for determining the total charge distributions at conductor-dielectric interfaces. This modification improved the method's accuracy.

Despite the advancements in the HBEM, the current version does not account for scenarios involving negligible conductor thickness, which is, as it already mentioned, a common approximation in microstrip designs. The main objective of this paper is to extend the HBEM to analyse microstrip structures with negligibly thin conductors, addressing a gap in existing quasi-static modelling techniques. The proposed approach enhances HBEM by introducing an improved charge distribution model, enabling more precise calculations of characteristic impedance and effective permittivity. This extension of HBEM will enable a more comprehensive solution, capable of analysing previously unaddressed structures.

The advantages of the enhanced HBEM will be presented through several illustrations, including assessments of computational efficiency and convergence analyses. The accuracy and efficiency of this method are validated through comparisons with the equivalent electrodes method (EEM) [20], finite element method (FEM) [21], and established literature data [22]. By incorporating the assumption of negligible thickness into the HBEM, this work offers a new tool for the analysis of microstrip lines, enhancing both accuracy and computational performance in practical applications.

The structure of the paper is as follows: after Introduction, section 2 presents the theoretical background of the extended HBEM. Section 3 discuss numerical results, including characteristic impedance and effective permittivity for single and coupled microstrip lines. The computational time, convergence of results, and comparisons with the other methods are also given in that section, followed by conclusions and insights for future research in section 4.

2. THEORETICAL BACKGROUND

A microstrip line with infinitely thin strip conductors, placed in an inhomogeneous area, above the infinite ground plane, is shown in Fig. 1.

According to the HBEM procedure, given in [18], the equivalent system is formed and shown in Fig. 2. Polarized line charges q'_{pim} ($i = 1, \dots, N-1$, $m = 1, \dots, M_i$) are placed in the air on separating surfaces between two layers of permittivity ε_i and ε_{i+1} ($i = 1, \dots, N-1$).

At the interface between the conductor and the dielectric layer, when the strip has a finite thickness, total charges, both free and polarized, are in the air, as described in [18].

However, with the strip now being of negligibly small thickness, the question arises of how and where to position the polarized charges. The top and bottom surfaces of the strip are in contact with different media, which resulting in distinct boundary conditions at these interfaces.

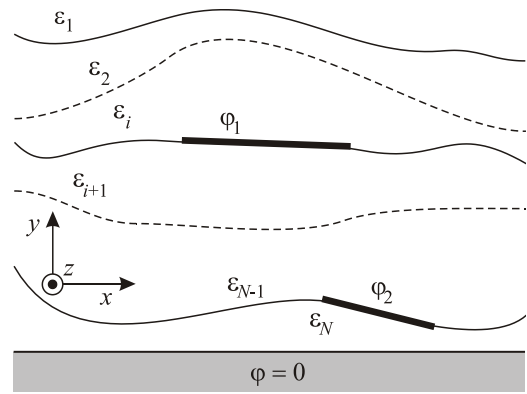


Fig. 1 – Microstrip line with infinitely thin strip conductors in inhomogeneous area.

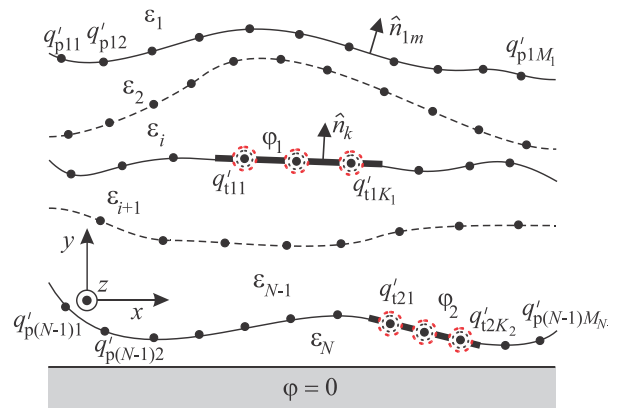


Fig. 2 – HBEM model.

The modification of the HBEM presented here involves introducing duplicate polarized charges on the strip, placed at identical locations alongside the free charges in the air, to satisfy the boundary conditions at the interface surfaces.

So, at strip surfaces total line charges exist,

$$q'_{tlk} = q'_{flk} + 2q'_{plk}, \quad (l = 1, 2, k = 1, \dots, K_l),$$

where indexes “f” and “p” correspond to the free and polarized (bound) charges, respectively.

In that way, the system of line charges above the infinite ground plane is formed. To determine the potential at any point of the system, the image theorem in the plane mirror should be applied, so the expression for the potential is

$$\begin{aligned} \varphi = & \sum_{l=1}^2 \sum_{k=1}^{K_l} \frac{q'_{tlk}}{4\pi\varepsilon_0} \ln \frac{(x - x_{lk})^2 + (y + y_{lk})^2}{(x - x_{lk})^2 + (y - y_{lk})^2} + \\ & + \sum_{i=1}^{N-1} \sum_{m=1}^{M_i} \frac{q'_{pim}}{4\pi\varepsilon_0} \ln \frac{(x - x_{im})^2 + (y + y_{im})^2}{(x - x_{im})^2 + (y - y_{im})^2}. \end{aligned} \quad (1)$$

The total number of unknowns is

$$N_{\text{tot}} = 3 \sum_{l=1}^2 K_l + \sum_{i=1}^{N-1} M_i. \quad (2)$$

At the boundary surfaces, between i -th and $(i+1)$ -th dielectrics, the boundary condition should be satisfied,

$$\hat{n}_{im} \cdot \mathbf{E}_{im}^{(0+)} = \frac{-\varepsilon_{i+1}}{\varepsilon_0(\varepsilon_i - \varepsilon_{i+1})} \eta_{pim}. \quad (3)$$

while between the conductor and i -th dielectric, the boundary condition has a form

$$\hat{\mathbf{n}}_k \cdot \mathbf{E}_k^{(0+)} = \frac{-\varepsilon_0}{\varepsilon_0(\varepsilon_i - \varepsilon_0)} \eta_{pk'} \quad (4)$$

where $\mathbf{E} = -\nabla(\varphi)$ represents the electric field strength vector, $\eta_{pim} = q'_{pim}/\Delta l_{im}$ and $\eta_{pk} = q'_{pk}/\Delta l_k$ are the surface charges on the segments of the lengths Δl_{im} (along two dielectric layers surface) and Δl_k (along separating surface between conductor and dielectric), respectively, ($i = 1, \dots, N-1$; $m = 1, \dots, M_i$; $k = 1, \dots, K_i$; $l = 1, 2$); $\hat{\mathbf{n}}_{im}$ and $\hat{\mathbf{n}}_k$ are the unit normal vectors oriented from the layer $i+1$ towards the layer i and from the conductor towards the layer i , respectively.

A program code is developed to facilitate the calculation of characteristic impedance and effective relative permittivity. The following procedure is applied:

- Position the equivalent electrodes (EEs) and form the HBEM model.
- Construct the system of linear equations by matching the conductor's potential using Eq. (1) and applying the boundary conditions at the separating surfaces using Eqs. (3) and (4).
- Solve the resulting system of linear equations.
- Determine the characteristic parameters – characteristic impedance and effective relative permittivity.

3. NUMERICAL RESULTS AND DISCUSSIONS

In this Section, the accuracy and efficiency of the HBEM are demonstrated through numerical simulations for both single and coupled microstrip lines. The results are compared with the EEM and FEM to validate the method's precision. Additionally, computational performance and practical applicability of HBEM are discussed.

To implement the procedure described in Section 2, a Mathematica code has been written to perform the numerical analysis of microstrip structures. The code automates the placement of equivalent electrodes, formulates and solves the system of equations, and extracts transmission parameters such as characteristic impedance and effective relative permittivity. This approach significantly reduces computational effort compared to traditional FEM simulations while maintaining high accuracy.

3.1 SINGLE MICROSTRIP LINE

A single microstrip line with negligible strip thickness is analyzed using HBEM. The structure, shown in Fig. 3, has the following parameters:

$$\varepsilon_{r1} = 1, \quad \varepsilon_{r2} = 16, \quad w/d = 2.0, \quad \text{and} \quad l/w = 6.0.$$

Applying the procedure described in Section 2, the results convergence and computation time for the characteristic impedance are shown in Fig. 4. The convergence study shows that HBEM achieves stable results within 100 seconds.

The developed Mathematica code was also used to compute the characteristic impedance for different w/d ratios. Those results are presented in Table 1, along with comparative values obtained from EEM, FEMM [21], and analytical solution [22]. The other parameters are:

$$\varepsilon_{r1} = 1, \quad \varepsilon_{r2} = 16, \quad l/w = 6.0 \quad \text{and} \quad t/d \rightarrow 0.$$

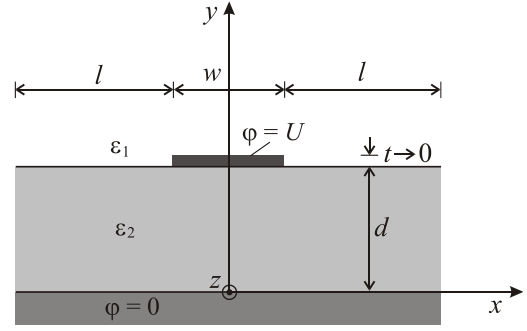


Fig. 3 – Single microstrip line.

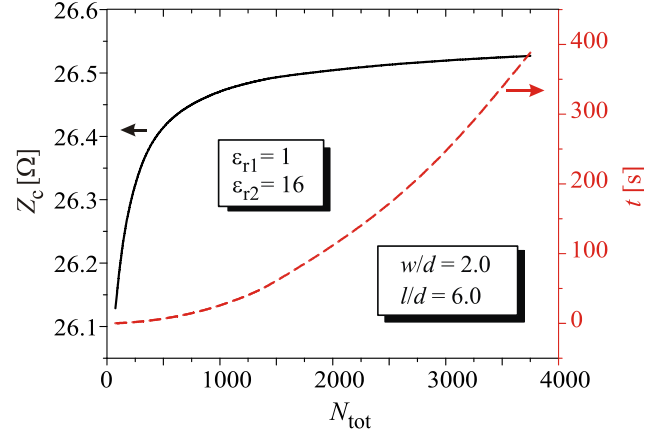


Fig. 4 – Results convergence and computation time.

Table 1
Characteristic impedance versus parameter w/d .

w/d	$Z_c [\Omega]$			
	HBEM	EEM	FEMM [21]	Analytical [22]
0.5	52.751	52.760	52.425	52.753
1.0	38.998	39.011	38.998	38.925
1.5	31.443	31.455	31.545	31.459
2.0	26.464	26.485	26.630	26.548
3.0	20.228	20.236	20.418	20.323
4.0	16.419	16.426	16.630	16.512

Increasing the strip width, the characteristic impedance decreases.

The maximum deviation between HBEM and other methods, calculated using

$$\delta[\%] = \left| \frac{Z_c^{\text{method}} - Z_c^{\text{HBEM}}}{Z_c^{\text{method}}} \right| \cdot 100, \quad (5)$$

is less than 1.3 %, as shown in Table 2, confirming the method's high accuracy. The label "method" corresponds to EEM, FEMM, and analytical solution, respectively.

Table 2
Results divergence, $\delta[\%]$.

w/d	method		
	EEM	FEMM [21]	Analytical [22]
0.5	0.017	0.621	0.004
1.0	0.033	0.879	0.187
1.5	0.038	0.323	0.051
2.0	0.079	0.623	0.316
3.0	0.039	0.930	0.467
4.0	0.043	1.269	0.563

Agreement with the EEM results is excellent, while deviations from the FEMM results stem from the mesh density used in the simulations. For the results presented, the number of elements in the constrained space during the problem modelling is approximately 700000.

Although the analysis considers the microstrip of infinite width, applying HBEM still requires selecting an appropriate width of the substrate. In this example, a ratio $l/w = 6.0$ is used. To explain that selection, the characteristic impedance as a function of the parameter l/w is analysed for different values of ϵ_{r2} , Fig. 5. This relationship reveals how changes in the electric properties of the substrate and the substrate's width influence the characteristic impedance.

It can be observed that for $l/w > 5.0$, a constant value of characteristic impedance is achieved, validating the choice of the l/w parameter. It can also be noticed that with an increase in the parameter ϵ_{r2} , the characteristic impedance values decrease.

The system depicted in Fig. 3 can also be solved using the EEM by applying the corresponding Green's function and the image theorem. However, the advantage of this improved version of HBEM compared to the EEM lies in its ability to determine the normalized distribution of polarized charges along both sides of the strip.

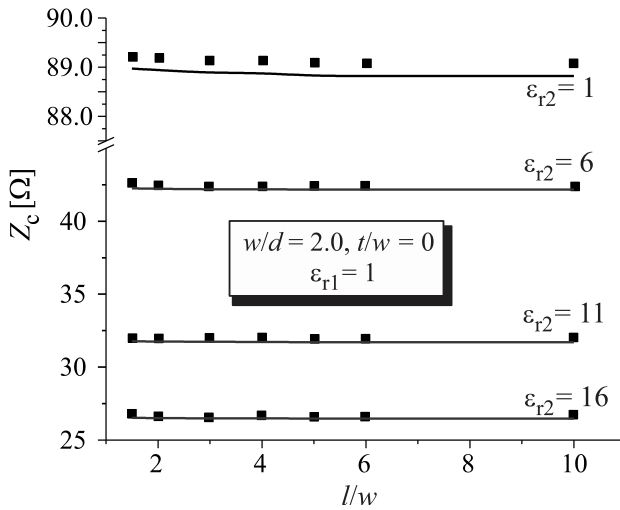


Fig. 5 – Characteristic impedance versus l/w for different values of the parameter ϵ_{r2} .

That distribution is presented in Fig. 6a. As is expected, there are no polarized charges along the side exposed to air.

The microstrip line dimensions are: $w/d = 2.0$, $l/w = 6.0$ and $t/d \rightarrow 0$.

If ϵ_{r1} differs from 1, for example $\epsilon_{r1} = 11$, the polarized charge distribution is shown in Fig. 6b.

3.2. COUPLED MICROSTRIP LINE

To further evaluate the applicability of HBEM, a coupled microstrip line structure, with negligible strips thicknesses, Fig. 7, of the following dimensions and parameters:

$\epsilon_{r1} = 1$, $\epsilon_{r2} = 16$, $w/d = 2.0$, $s/w = 0.5$, and $l/w = 6.0$, is presented.

Both, the even and odd, modes will be analysed. Given that this system can be considered symmetric (for the even mode) and axisymmetric (for the odd mode), it suffices to analyse only one half of the system. This approach reduces calculation time and enhances both accuracy and convergence of results, as shown in Fig. 8. For the following calculations, the number of unknowns will be set to 600.

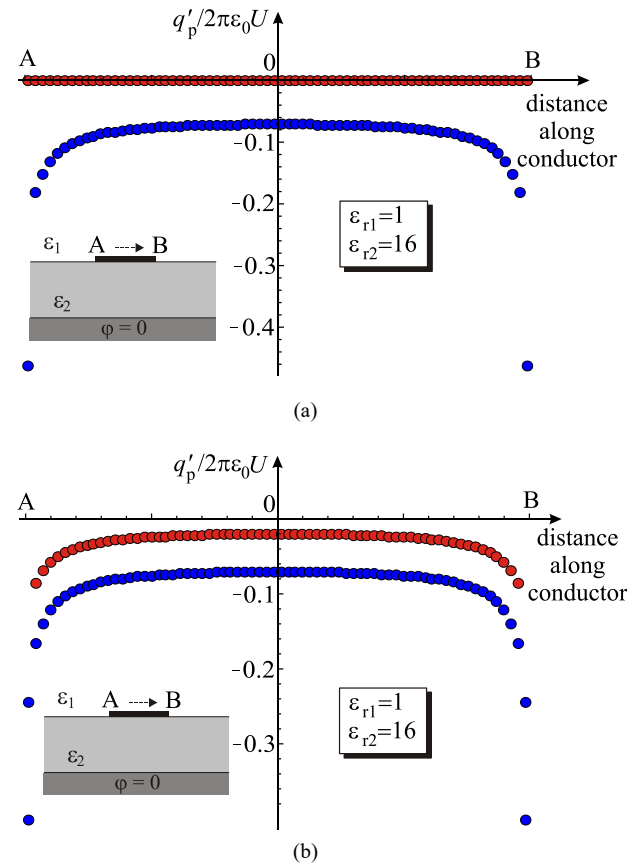


Fig. 6 – Normalized polarized line charges distribution along the strip for: (a) $\epsilon_{r1} = 1$ and (b) $\epsilon_{r1} = 11$.

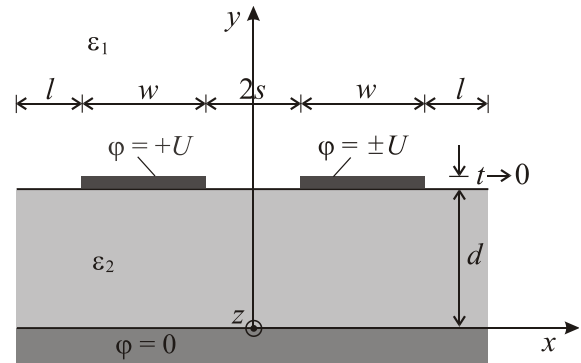


Fig. 7 – Coupled microstrip lines.

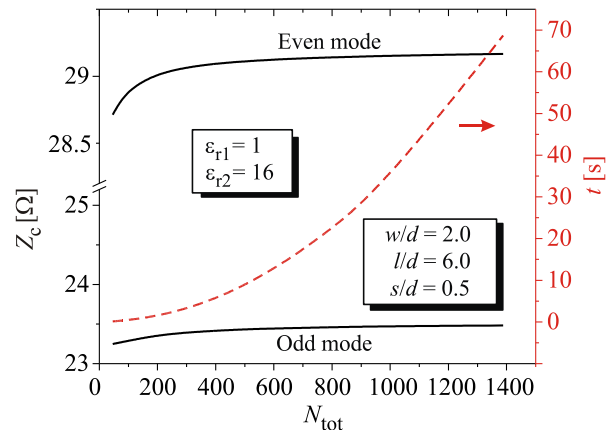


Fig. 8 – Results convergence and computation time.

The results for characteristic impedance as a function of strip width are shown in Tables 3 and 4.

Table 3

Characteristic impedance versus parameter w/d – Even mode.

w/d	$Z_c [\Omega]$		
	HBEM	EEM	FEMM [21]
0.5	60.157	60.158	59.089
1.0	43.866	43.869	43.455
1.5	34.928	34.928	34.817
2.0	29.119	29.117	29.324
3.0	21.931	21.926	22.099
4.0	17.624	17.617	17.852

Table 4

Characteristic impedance versus parameter w/d – Odd mode.

w/d	$Z_c [\Omega]$		
	HBEM	EEM	FEMM [21]
0.5	45.004	45.015	44.557
1.0	33.704	33.714	33.316
1.5	27.536	27.544	27.078
2.0	23.439	23.445	23.350
3.0	18.205	18.208	18.061
4.0	14.953	14.954	14.894

A close match with the EEM and FEMM results is achieved. With an increase in strip width, the characteristic impedance decreases for both modes.

How does the distance between the strips, s/d , affect the values of characteristic impedance and effective relative permittivity? This is illustrated in Fig. 9, where an additional variable parameter is the substrate relative permittivity, ϵ_{r2} . Values for the even mode are shown with solid black lines, while those for the odd mode are shown with red dashed lines.

Regarding the characteristic impedance, as the distance between the strips increases, its value decreases for the even mode and increases for the odd mode. It can also be observed that with an increase in the parameter ϵ_{r2} , the characteristic impedance values decrease for both modes.

Effective relative permittivity for the even mode decreases with increasing the distance between the strips, but for the odd mode increases. With an increase in substrate permittivity, the effective relative permittivity rises for both modes.

The normalized distribution of the polarized charges along the right conductor is shown in Fig. 10 for both the even and odd modes. The microstrip line dimensions for these calculations are:

$$w/d = 2.0, l/w = 6.0 \text{ and } t/d \rightarrow 0.$$

As already observed in Fig. 6a, it is evident that there are no polarized charges in the air, while those charges are present in the dielectric layer.

Their values are negative for the even mode, while they are positive when the right conductor is at the negative potential, $\varphi = -U$.

The ability to model polarized charge distributions along the conductors provides insights into field interactions, which are difficult to obtain with FEM as well as EEM.

4. CONCLUSIONS

This study presents an extended hybrid boundary element method (HBEM) for analysing microstrip lines with negligible metallization thickness.

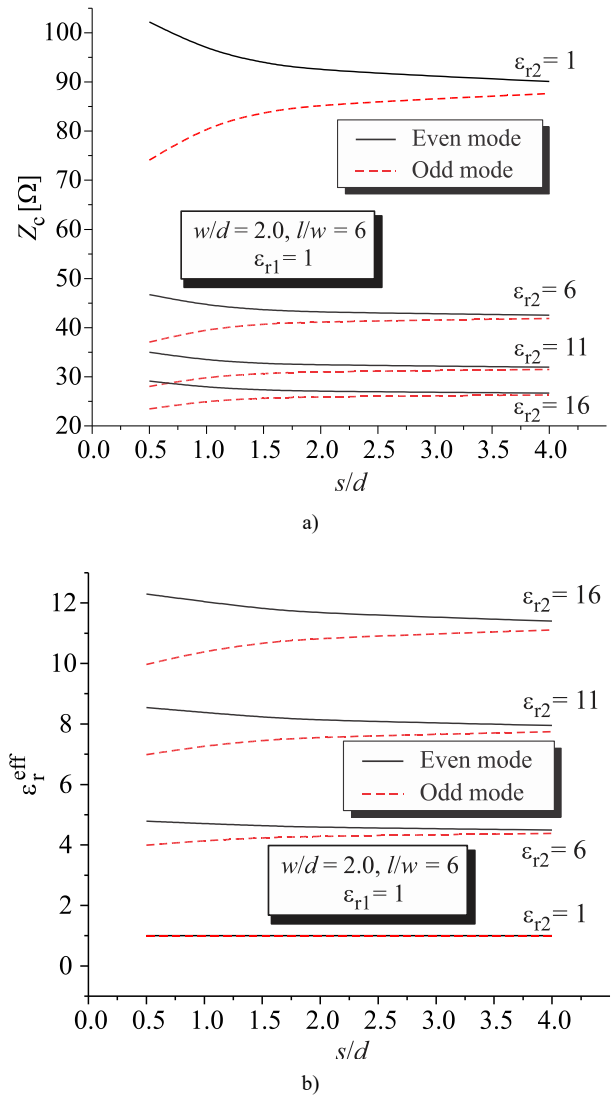


Fig. 9 – (a) Characteristic impedance and b) effective relative permittivity versus s/d for different values of parameter ϵ_{r2} .

The modified HBEM effectively determines essential transmission parameters, such as characteristic impedance and effective relative permittivity, in cases of minimal strip conductor thickness.

Comparison with the equivalent electrodes method (EEM) and finite element method (FEM) confirms strong agreement, underscoring the accuracy and computational efficiency of this approach. The results indicate that the extended HBEM is an easy to implement solution for analysing microstrip lines using the quasi-static approach. Also, compared with the other numerical simulation, it saves a lot of repetitive modelling time and computational resources.

The development of Mathematica-based numerical implementation further enhances the practicality of HBEM for analyzing different microstrip configurations.

This method's adaptability and precision suggest significant potential for practical applications in microwave and millimeter-wave circuit designs. Future research may extend this approach to complex dielectric configurations and further explore its applicability to other electromagnetic structures with negligibly thin conductors.

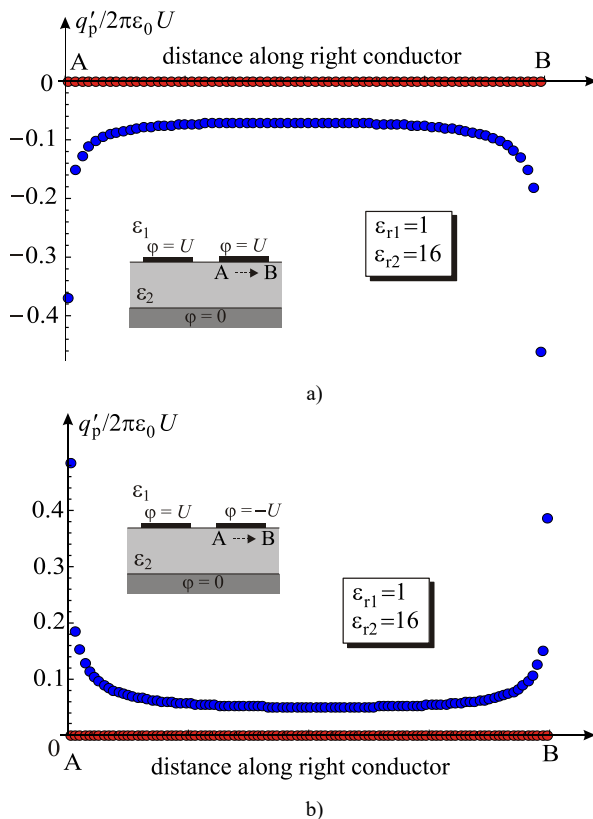


Fig. 10 – Normalized polarized line charges distribution along the right strip for: (a) Even and (b) Odd mode.

ACKNOWLEDGEMENT

This work has been supported by the Ministry of Science, Technological Development and Innovation of the Republic of Serbia [Grant Number: 451-03-137/2025-03/200102]

The authors would like to extend their sincere appreciation to Dr. Saša S. Ilić for the valuable comments and insightful suggestions provided during our previous scientific work, which significantly enhanced the quality of our research.

CREDIT AUTHORSHIP CONTRIBUTION

Mirjana Perić: methodology, investigation, data curation, software, visualisation, and writing – original draft.

Ana Vučković: methodology, software, and editing.

Nebojša Raičević: methodology, validation, and supervision.

Received on 15 November 2024.

REFERENCES

1. M. Nicolaescu, V. Croitoru, L. Tuță, *Transient analysis of a*

2. X. Fan et al., *A filtering switch made by an improved coupled microstrip line*, Applied Sciences, **13**, 13, p. 7886 (2023).
3. P. Jha, A. Kumar, N. Sharma, *Metamaterial-inspired split ring resonator accomplished multiband antenna for 5G and other wireless applications*, Rev. Roum. Sci. Techn., **68**, 2, pp. 127–131 (2023).
4. T.G. Bryant, J.A. Weiss, *Parameters of microstrip transmission lines and of coupled pairs of microstrip lines*, IEEE Trans. Microwave Theory Tech., **16**, 12, pp. 1021–1027 (1968).
5. J. Nagel, *An analytic model for stripline/microstrip potential using infinite series with mixed boundary conditions*, Progress in Electromagnetics Research M, **107**, pp. 231–242 (2022).
6. K. Biswas, *A study and analysis on simple microstrip line*, Int. Journal of All Research Education and Scientific Methods (IJARESM), **12**, 6, pp. 888–891 (2024).
7. A. Shadare, M. Sadiku, S. Musa, *Markov chain Monte Carlo analysis of microstrip line*, International Journal of Engineering Research and Advanced Technology, **2**, 3, pp. 11–17 (2016).
8. M. Hayati et al., *A study in characteristic impedance of a microstrip transmission line by COMSOL model*, Int. Journal of Natural and Engineering Sciences, **6**, 3, pp. 59–62 (2012).
9. S. Bishwakarma, A. Kumar, K.B. Singh, *Study of dispersion analysis for various microstrip line configurations using finite difference method*, International Journal of Scientific Research in Science and Technology, **9**, 6, pp. 56–63 (2022).
10. S.D. Lin, S. Pu, C. Wang, H.Y. Ren, *Compact design of annular-microstrip-fed mmW antenna arrays*, Sensors, **21**, 11, p. 3695 (2021).
11. T-N. Chang, C-H. Tan, *Analysis of a shielded microstrip line with finite metallization thickness by the boundary element method*, IEEE Trans. Microwave Theory Tech., **38**, 8, pp. 1130–1132 (1990).
12. S. Woo, et al., *Analysis of microstrip line with asymmetric arch type cross-sectional structure using micro pattern transfer printing method*, Sensors, **22**, 15, 5613 (2022).
13. M. Perić, S. Aleksić, A. Vučković, *Influence of metallization thickness on microstrip lines characteristic parameters distribution*, The 17th International IGTE Symposium, pp. 71–76 (2016).
14. N. Raičević, S. Aleksić, S. Ilić, *A hybrid boundary element method for multi-layered electrostatic and magnetostatic problems*, Journal of Electromagnetics, **30**, pp. 507–524 (2010).
15. N. Raičević, S. Ilić, S. Aleksić, *Application of new hybrid boundary element method on the cable terminations*, 14th International IGTE Symposium, pp. 56–61 (2010).
16. A. Vučković, D. Vučković, M. Perić, N. Raičević, *Influence of the magnetization vector misalignment on the magnetic force of permanent ring magnet and soft magnetic cylinder*, International Journal of Applied Electromagnetics and Mechanics, **26**, pp. 417–430 (2021).
17. S. Ilić, M. Perić, S. Aleksić, N. Raičević, *Hybrid boundary element method and quasi-TEM analysis of 2D transmission lines - generalization*, Electromagnetics, **33**, 4, pp. 292–310 (2013).
18. M. Perić, S. Ilić, A. Vučković, N. Raičević, *Improving the efficiency of hybrid boundary element method for electrostatic problems solving*, ACES journal, **35**, 8, pp. 872–877 (2020).
19. S. Ilić, N. Raičević, S. Aleksić, *Application of new hybrid boundary element method on grounding systems*, 14th International IGTE Symposium, pp. 160–165 (2010).
20. D.M. Veličković, *Equivalent electrodes method*, Scientific Review, **21–22**, pp. 207–248 (1996).
21. D. Meeker, Software package FEMM, ver. 4.2, available online at: <http://www.femm.info/wiki/Download> (accessed 20 July 2024).
22. ***Microstrip Line Calculator, available at: <https://www.emtalk.com/mscalc.php> (accessed 26 August 2024).